NEUROBOTICS Meeting

Genova, September 22, 2005

# A Bio-Inspired Sensory-Motor Neural Model for a Neuro-Robotic Manipulation Platform


Gioel Asuni, Giancarlo Teti, Cecilia Laschi, Eugenio Guglielmelli and Paolo Dario

ARTS Lab (Advanced Robotics Technology and System Laboratory)

Scuola Superiore Sant'Anna, Pisa, Italy


Scuola Superiore Sant'Anna di Studi Universitari e di Perfezionamento

ARTS Lab Advanced Robotics Technology and Systems Laboratory

# Objective of my research

Design and Development of
**modular system**
able to
**generate**, **control** and **coordinate**
robotic platform **movements**
in order to
**reach** and stable **grasp** a object

# Motivation

To **generate**, **control** and **coordinate** the **movements** of increasingly complex, difficult to model, and reconfigurable biorobotic systems

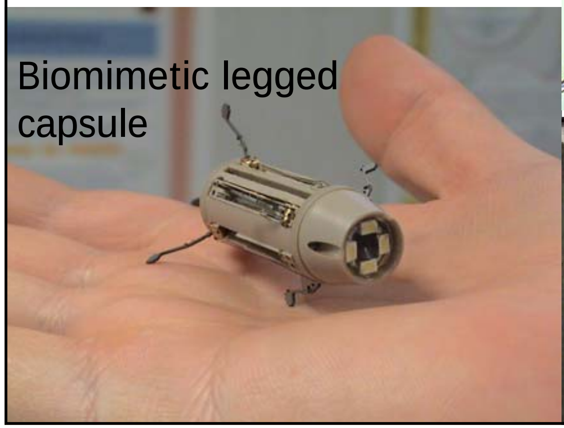

Biomimetic legged capsule

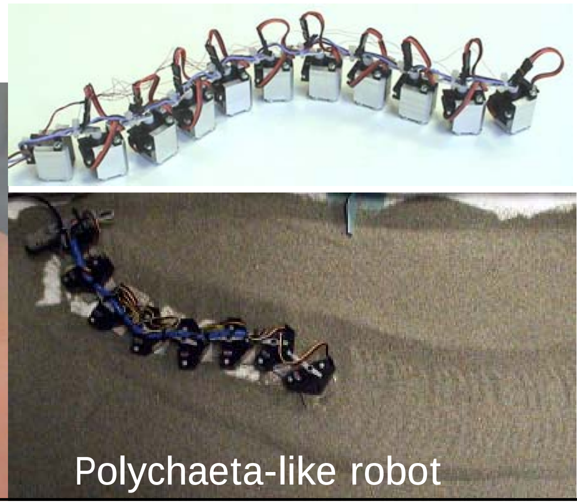

Polychaeta-like robot

Human-like upper body

# The robotic platform

**Anthropomorphic head & retina-like vision system**

- 7 d.o.f.s (neck & eyes)
- 7 proprioceptive sensors
- 2 cameras

**Anthropomorphic arm**

- 8 d.o.f.s
- 16 proprioceptive sensors

**Biomechatronic hand**

- 10 d.o.f.s
- 16 proprioceptive sensors
- 9 tact. sensors

**Total**

- d.o.f.s: 25
- Visual sensors: 2
- Proprioceptive sensors: 39
- Tactile sensors: 9

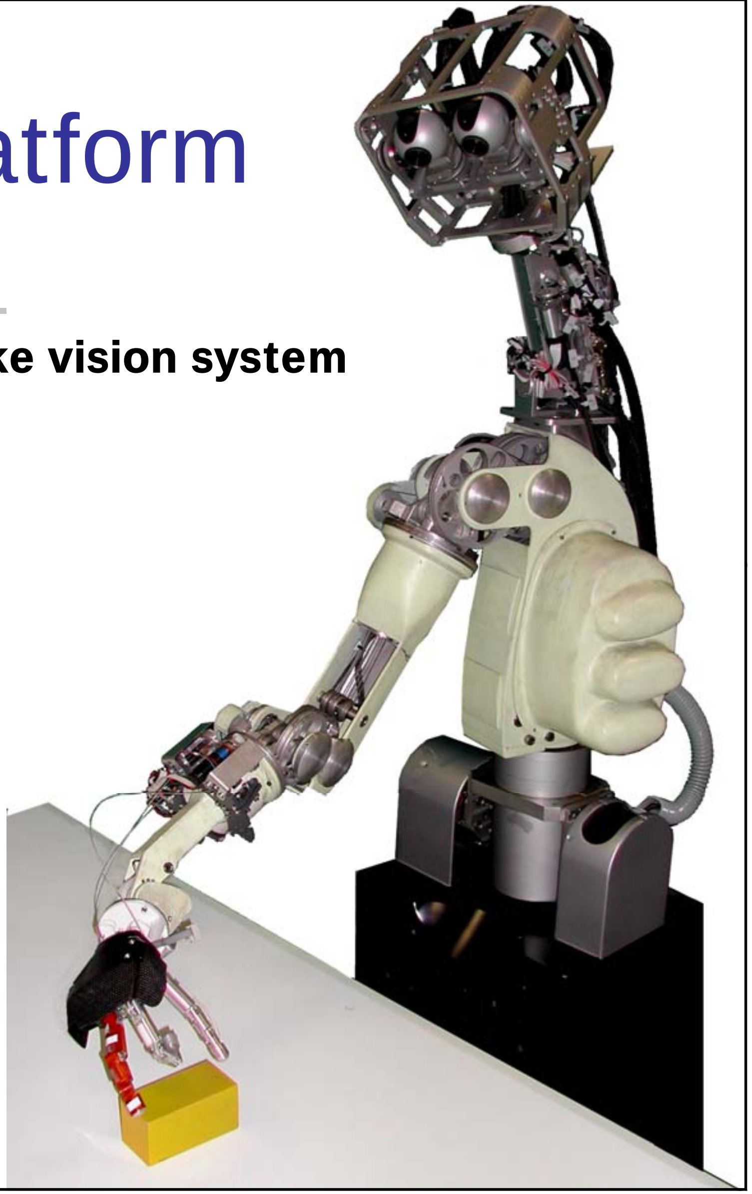

# The head

**Head**

7 d.o.f.s (neck: 4 d.o.f.s, eyes: 3 d.o.f.s)

Dimensions: neck, 200x100x100 mm
head, 180x200x150 mm

Weight: about 5.3 Kg

Intraocular distance: variable from 60 to 100 mm.

Ranges of motion and speeds:

- Eye Pitch Axis: ±47°, 600°/s
- Eye R/L Yaw Axis: ±45°, 1000°/s
- Yaw: ±100°, 170°/s
- Roll: ±30°, 25°/s
- Upper Pitch: ±30°, 120°/s
- Lower Pitch: ±25°, 20°/s

Ocular movements: saccades, smooth pursuit, and vergence

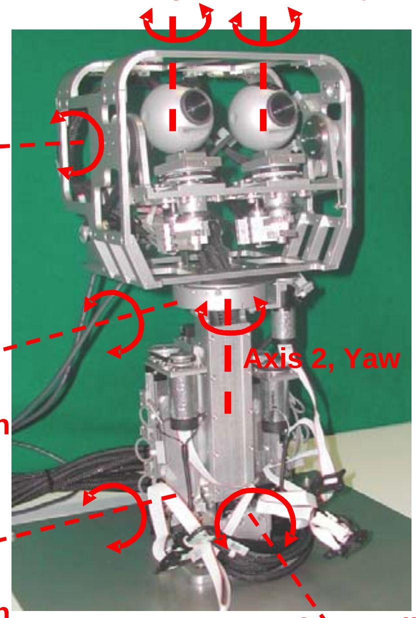

# The Dexter Arm

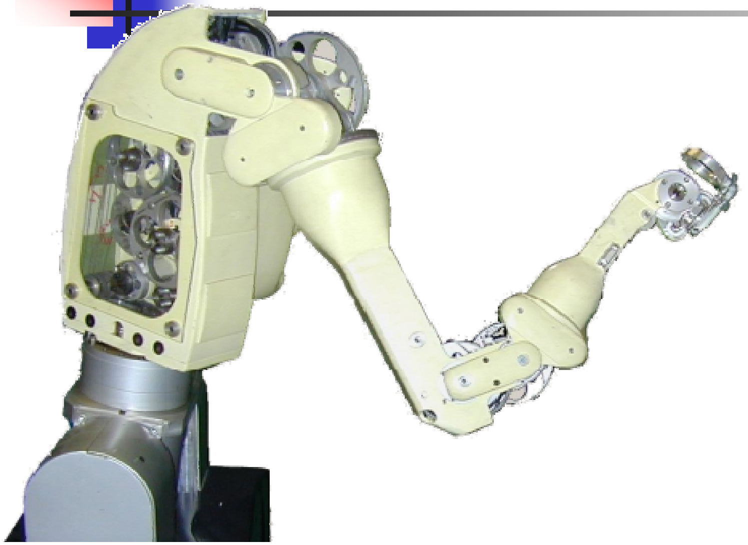

| | |
|---|---|
| D.o.f.: | 8 |
| Velocity: | 0.2 m/s |
| Workspace: | 1200 mm x 350° |
| Repeatability: | $\pm$ 1mm |
| Weight: | 40 Kg |
| Payload: | 2 Kg |
| Power: | 24V DC |

- 8-d.o.f. anthropomorphic redundant robot arm, composed of trunk, shoulder, elbow and wrist
- mechanically coupled structure: the mechanical transmission system is realized with pulleys and steel cables
- main characteristics: reduced accuracy,lighter mechanical structure, safe and intrinsically compliant structure

# The hand

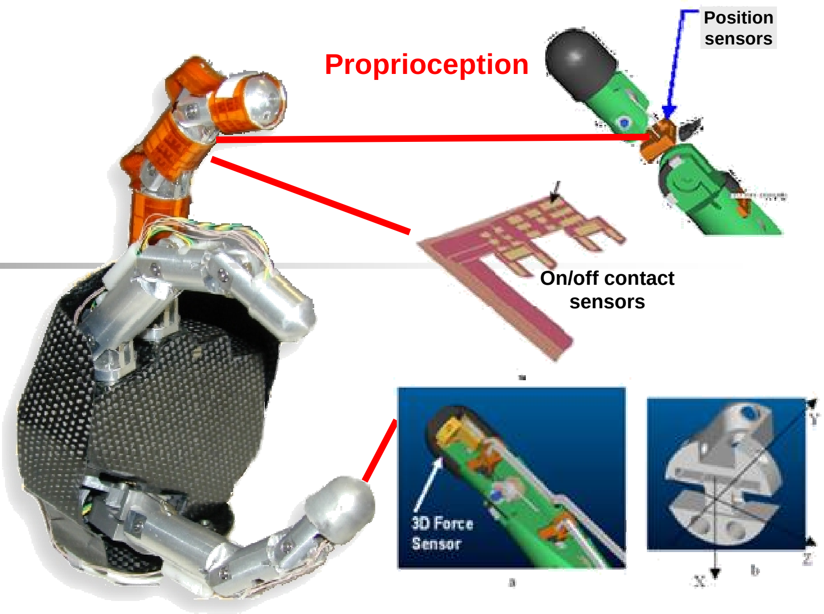


### Hand mechanical specifications

10 d.o.f.s; 6 underactuated, 4 motor actuat.

- three identical underactuated 3 dof fingers with cylindrical phalanges, driven by a single cable allowing flexion/extension
- a 2 DoFs trapezo-metacarpal joint at the base of the palm allowing thumb opposition movement (adduction/abduction) towards the other 2 fingers

Weight: about 400gr

Dimension: similar to the human hand

### Performances

- trapezo-metacarpal thumb joint abduction/adduction range: 0°-120°
- finger joints flexion range: 0-90°
- load weight: 450 gr
- grasping force: 40 N
- tip to tip force: 15 N
- closing time: 2 sec.

### Proprioceptive System

- 3 position Hall-effect sensors, one per phalanx, for each finger
- 4 motor encoders
- 3 force tension sensors providing the tension of the actuation cable

### Tactile System

- a 3D force sensor for each finger embedded in the fingertip providing the three force components of the contact
- 9 ON/OFF contact sensors for each finger:
  - 1 on the distal phalange
  - 1 on the intermediate phalanx
  - 1 on the proximal phalanx

# Outline of the talk

- Objective of the work: to simplify the control of goal-oriented reaching for robotic arms by taking inspiration from neuroscience
- Proposed model: a self-organizing neural controller
- Implementation tools: Growing Neural Gas Networks
- Experimental trials and results
- Conclusions

# Addressed Problem

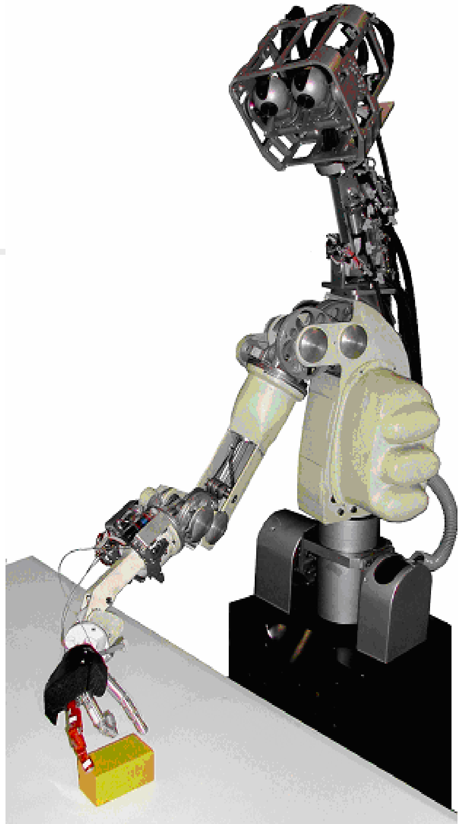

To develop a control module that receives in input a target 3D position and provides in output a command sequence able to reach it

Target 3D Position
$(X_t, Y_t, Z_t)$

?

Motor Command
$\{(J0_i, \ldots, J7_i)\}$

ARM

# Traditional solutions

Based on mathematical computational models such as **inverse transform** or **iterative methods**

Drawbacks (especially when the number of DOF increases):

- Inverse transform does not always guarantee a closed-form solution (numerical problems – matrix inversion)
- Iterative methods may not converge and may be computationally expensive

Both of the forms are generally rigid and do not account for uncontrollable variables such as manufacture tolerances, calibration error, and wear

**Kinematic inversion**
Ramdane-Cherif, A.; Daachi, B.; Benallegue, A.; Levy, N.;
Intelligent Robots and System, 2002. IEEE/RSJ International Conference on
Volume 2, 30 Sept.-5 Oct. 2002 Page(s):1904 - 1909 vol.2

**Inverse kinematic at acceleration level using neural network**
Ramdane-Cherif, A.; Perdereau, V.; Drouin, M.;
Neural Networks, 1995. Proceedings., IEEE International Conference on
Volume 5, 27 Nov.-1 Dec. 1995 Page(s):2370 - 2374 vol.5

## Proposed approach

### Neural models

- no a priori knowledge on kinematic and mechanical structure is required (e.g. link length, link structure)
- *learning* capability, to develop an internal model that builds such knowledge
- low computational complexity
- human-like flexibility, robustness, generalization

## A good starting point: the DIRECT model

## The proposed model

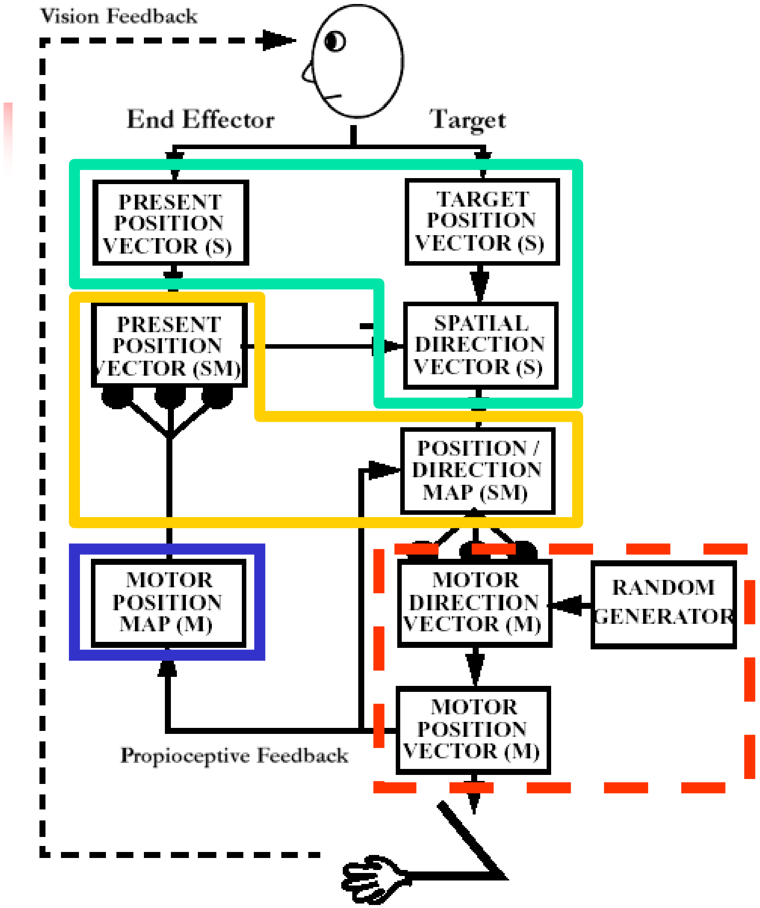


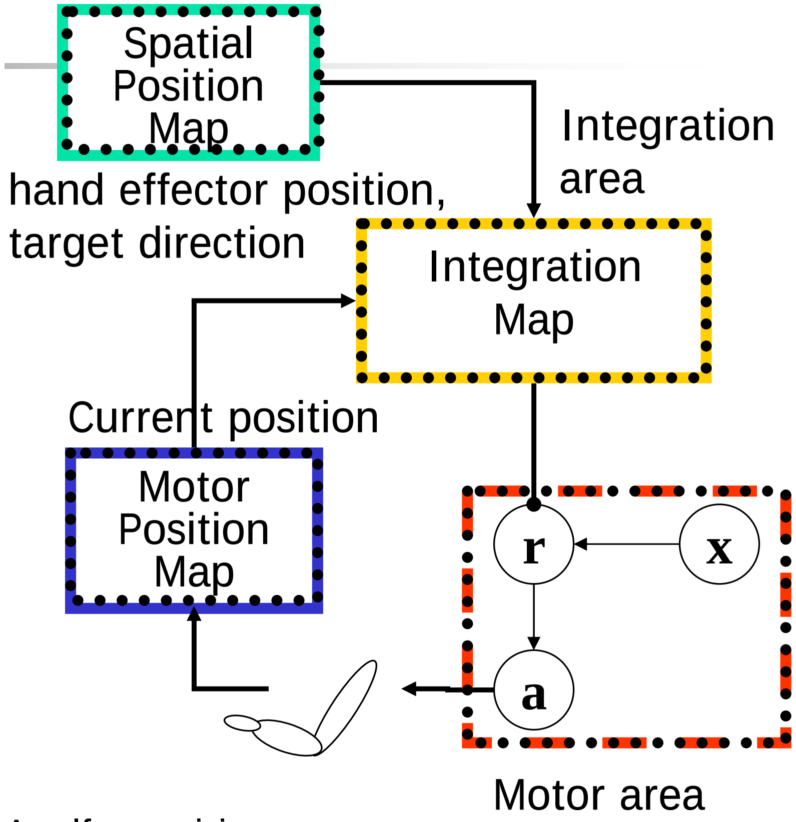


**Bullock**, D., **Grossberg**, S., **Guenther**, F. H. (1993). "A self-organizing neural model of motor equivalent reaching and tool use by a multijoint arm." *Journal of Cognitive Neuroscience, 5, 408-435.*

# The proposed neural model

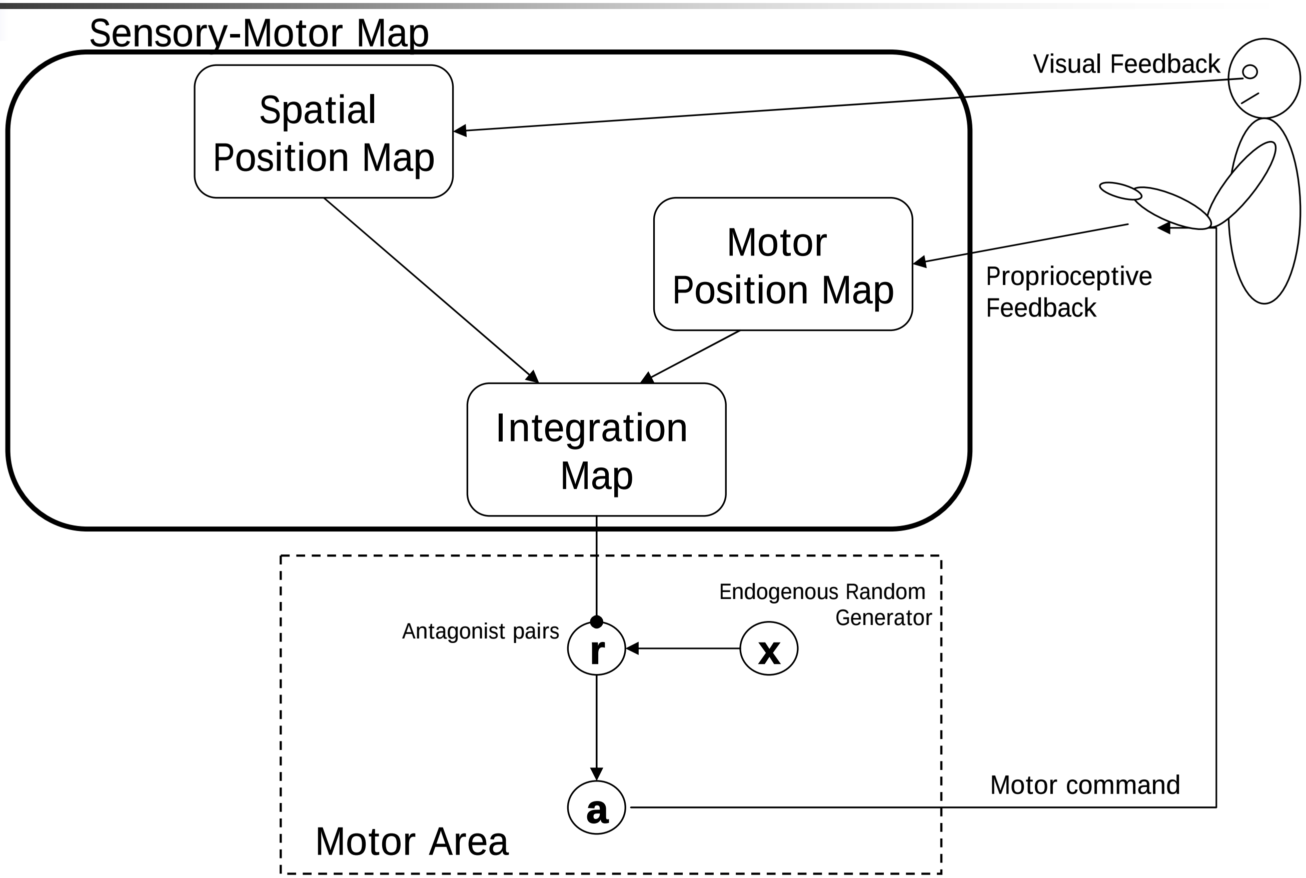

Each joint is actuated by simulating a pair of agonist-antagonist muscles, including a spring-like mechanism

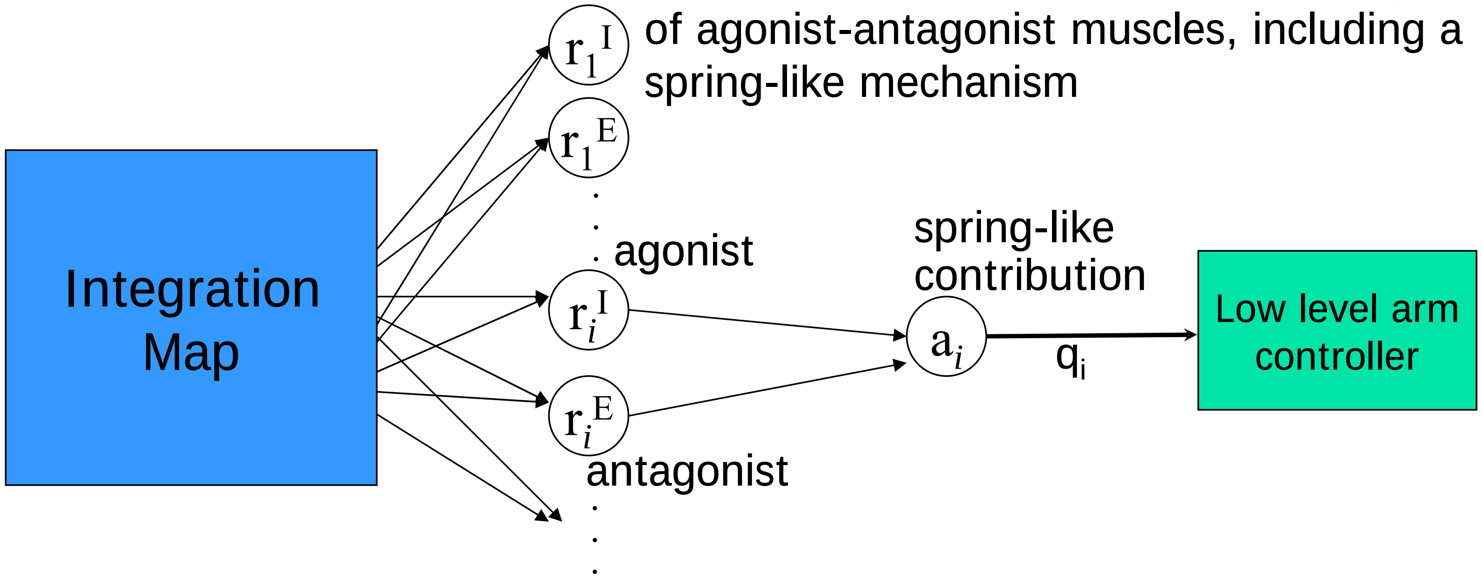


The Integration Map (IM) has two-fold functionality:

- Sensory: it combines different information
- Motor: it provides an activation pattern of cells (**r**) in order to perform a movement in a given direction

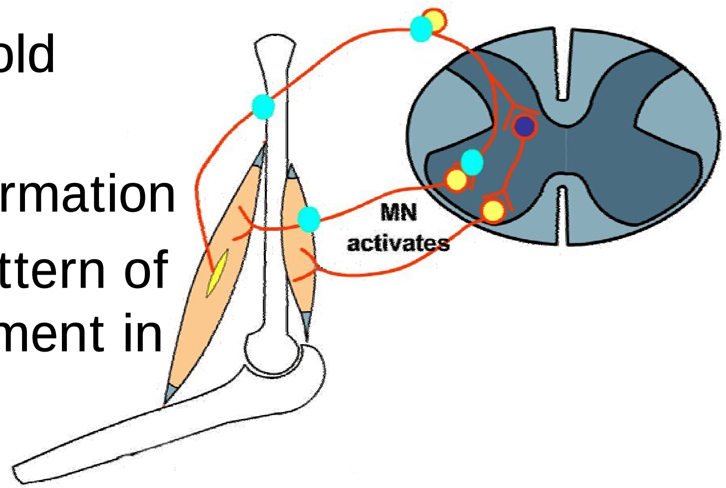

# Implementation tools: Growing Neural Gas Networks

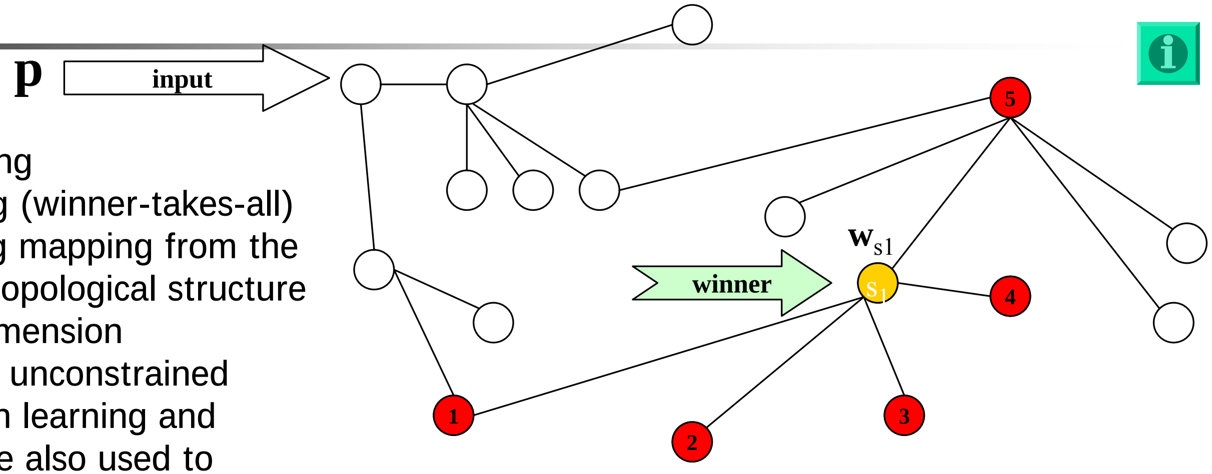


- Unsupervised learning
- Competitive learning (winner-takes-all)
- Topology-preserving mapping from the input space onto a topological structure of equal or lower dimension
- Network topology is unconstrained
- Competitive Hebbian learning and connection aging are also used to generate the topology
- Growth mechanism (the network size need not be predefined)
- The growth process can be interruped when a user defined performance criterion has been fulfilled

$\mathbf{w}_i$ is the weight vector associated to the unit $i$

Set of direct topological neighbors of the winner unit ($S_1$)

$$N_{s1} = \{ 1 \; 2 \; 3 \; 4 \; 5 \}$$

Updating rules:

$$\mathbf{w}_{s1} = \mathbf{w}_{s1} + \varepsilon_b (\mathbf{p} - \mathbf{w}_{s1})$$

$$\mathbf{w}_i = \mathbf{w}_i + \varepsilon_n (\mathbf{p} - \mathbf{w}_i) \; (\forall i \in N_{s_1})$$

**Bernd Fritzke**, "Growing Cell Structures - A Self-organizing Network for Unsupervised and Supervised Learning". ICSI TR-93-026, 1993. *Neural Networks* 7(9):1441-1460, 1994a

# Experimental setup

- Manipulators:
  - 2D Simulator – 3 d.o.f
  - DEXTER arm – 8 d.o.f.
  - PUMA560 arm – 6 d.o.f
- A simulator vision system:
  - by direct kinematics
- Training phase (motor babbling):
  - by autonomously generated repetitions of an action-perception loop
- Testing:
  - Reaching a given target point:
    - in normal condition
    - with a tool
    - with clamped joint
    - vision distortion
    - blind reaching

# Experimental results: 2D simulator

3 planar joints

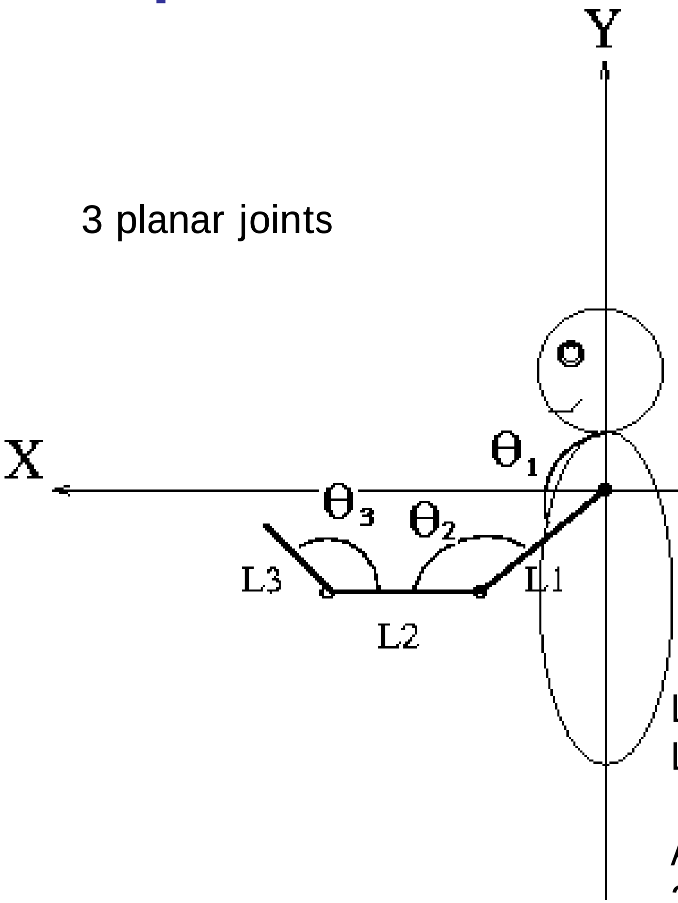


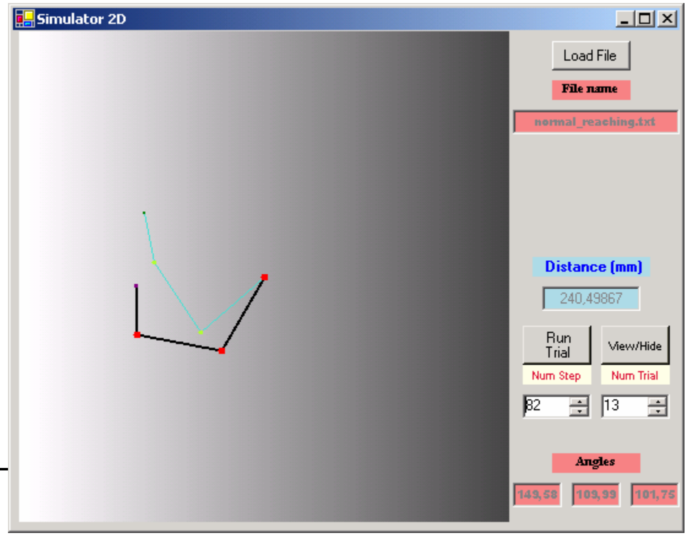


**Graphical interface**

Lengths ranges:

$L_1$= 280 mm $L_2$= 280 mm $L_3$= 160 mm

Angle ranges:

$30° \leq \Theta_1 \leq 240°$ $30° \leq \Theta_2 \leq 180°$ $30° \leq \Theta_3 \leq 190$

# 2D simulation: Normal reaching

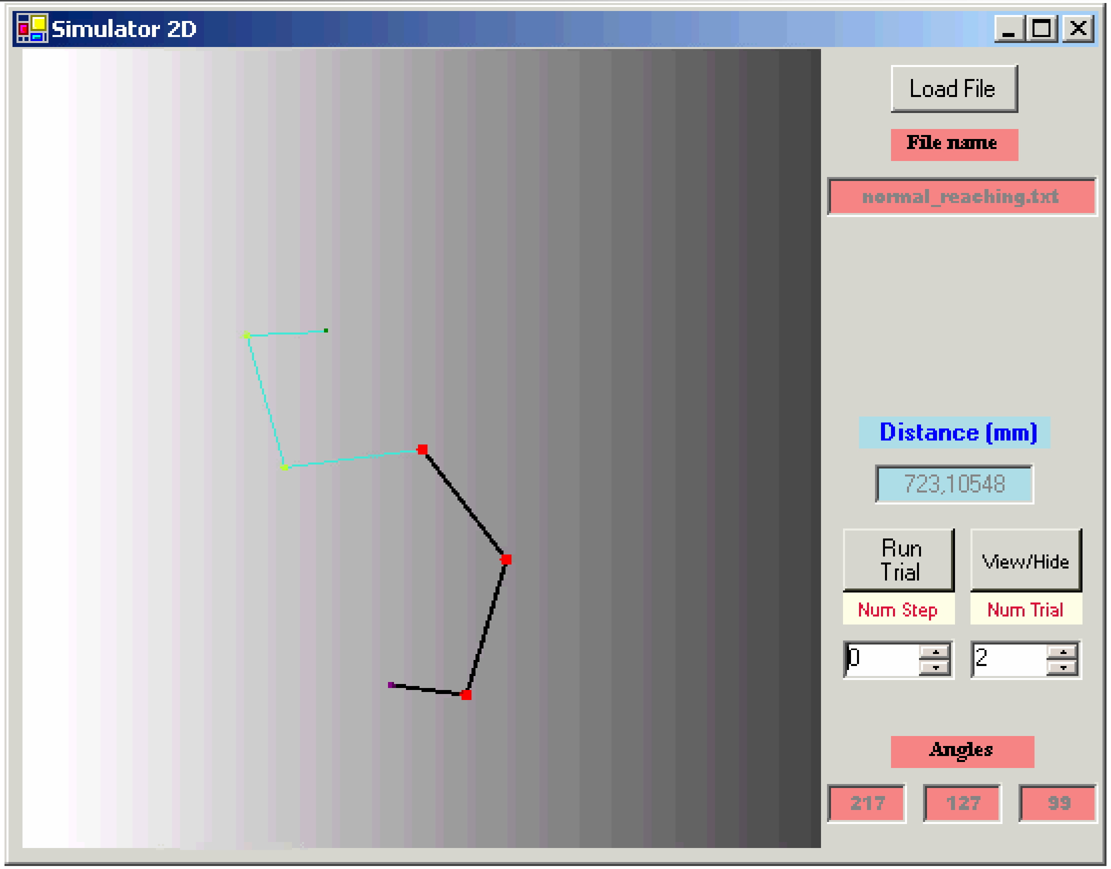

# Experimental results: 2D simulator

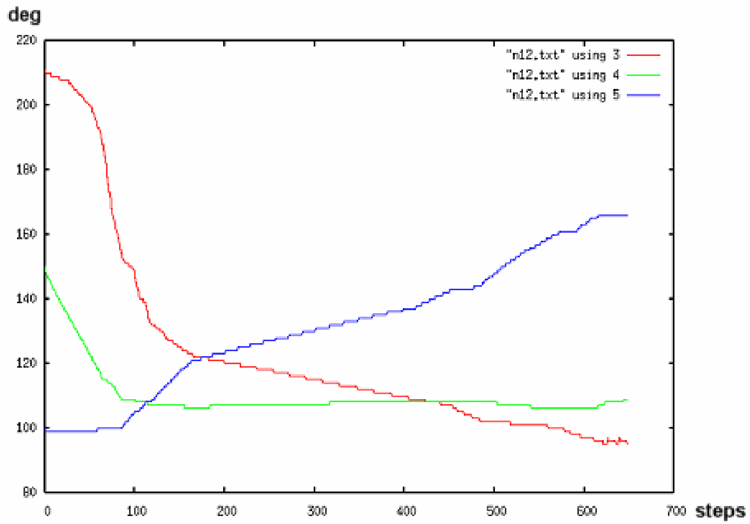


the **joint trajectories** in a normal reaching task: no oscillations

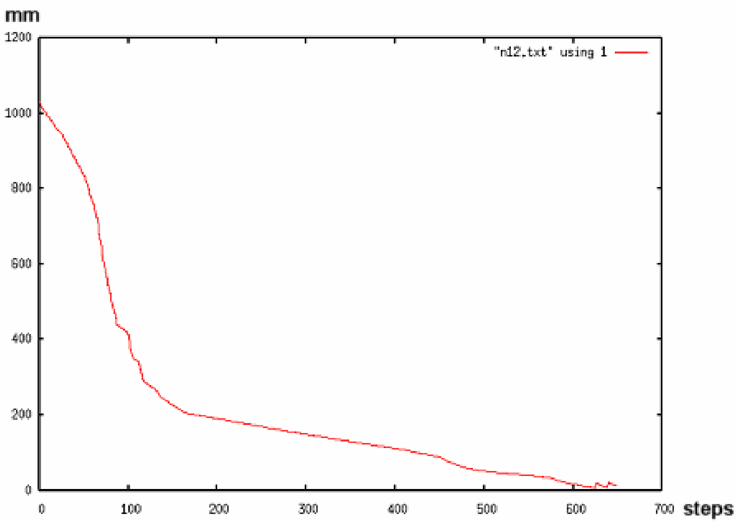


graph of the **error distance** between the end-effector and the target: monotonic trend

**Cardinality of the obtained maps**

| | Visual Map | Postural Map | Sensory Motor Map |
|---|---|---|---|
| Our model | 2369 | 1333 | 3357 |
| DIRECT model | – | 15625 | 10290 |

## Human-like flexibility and robustness in reaching tasks provided by the model

The model, after learning occurs, produces linear end-effector trajectories and human-like movement behaviors such as:

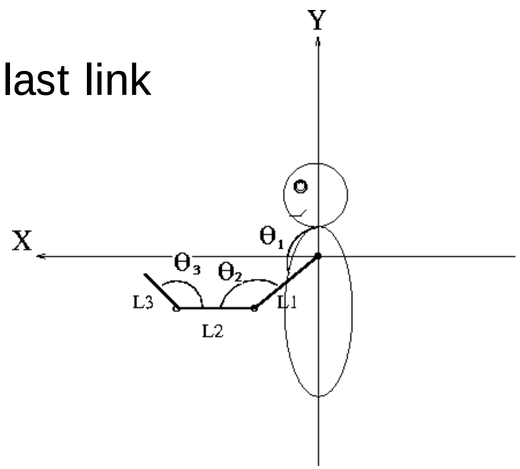


*reaching with a tool*

adding a tool of variable length at the end of last link

*clamped joint*

reaching tasks with a clamped joint

*vision distortion*

using a prism that allows a visual shift

*blind reaching*

reaching without using any visual feedback

**without additional learning, or corrective movements**

# Experimental results: 2D simulation - Reaching with a tool

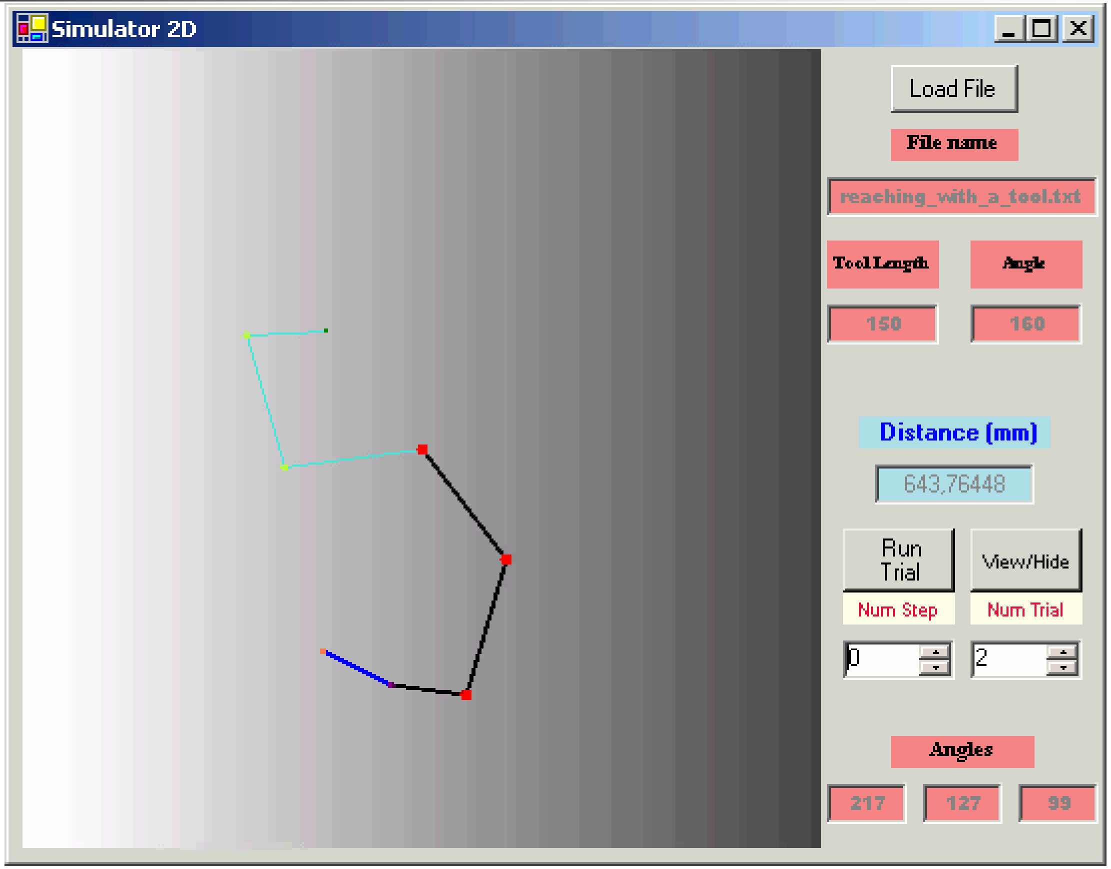

# Experimental results: 2D simulation - Clamped joint

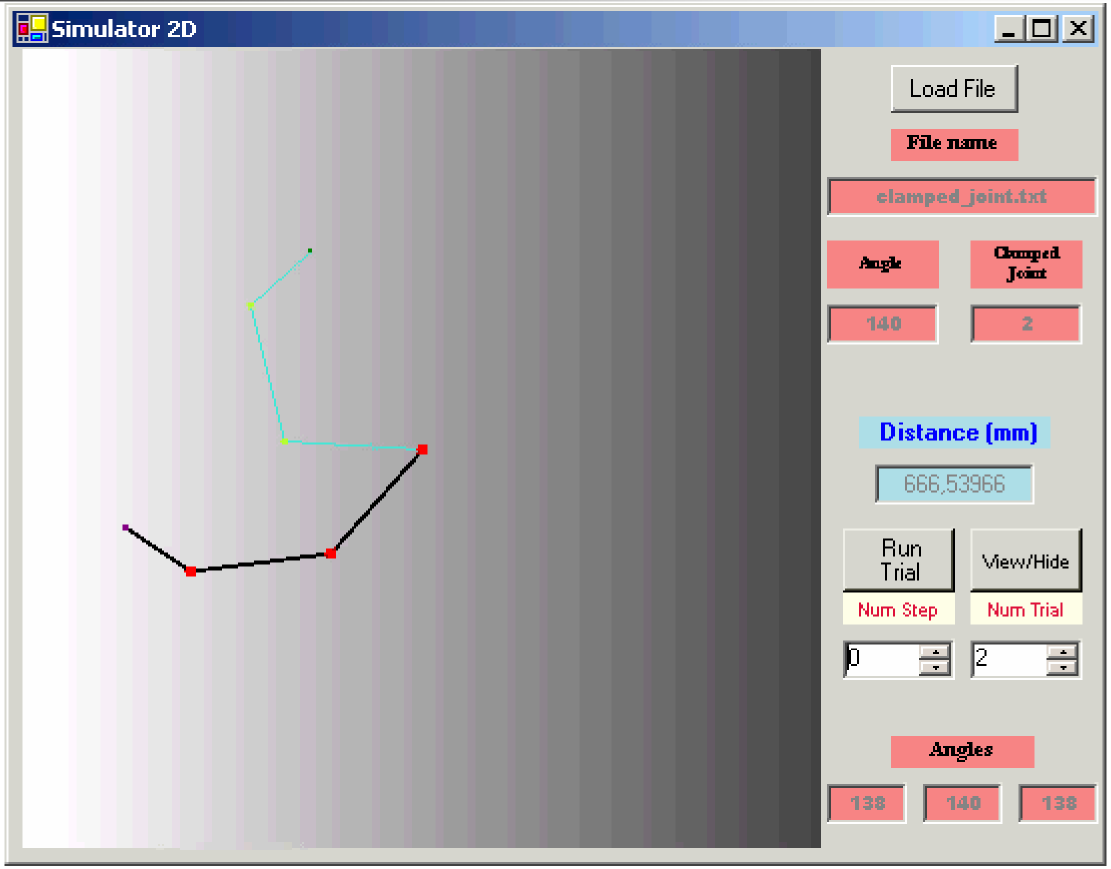

# Experimental results: 2D simulation - Visual shift

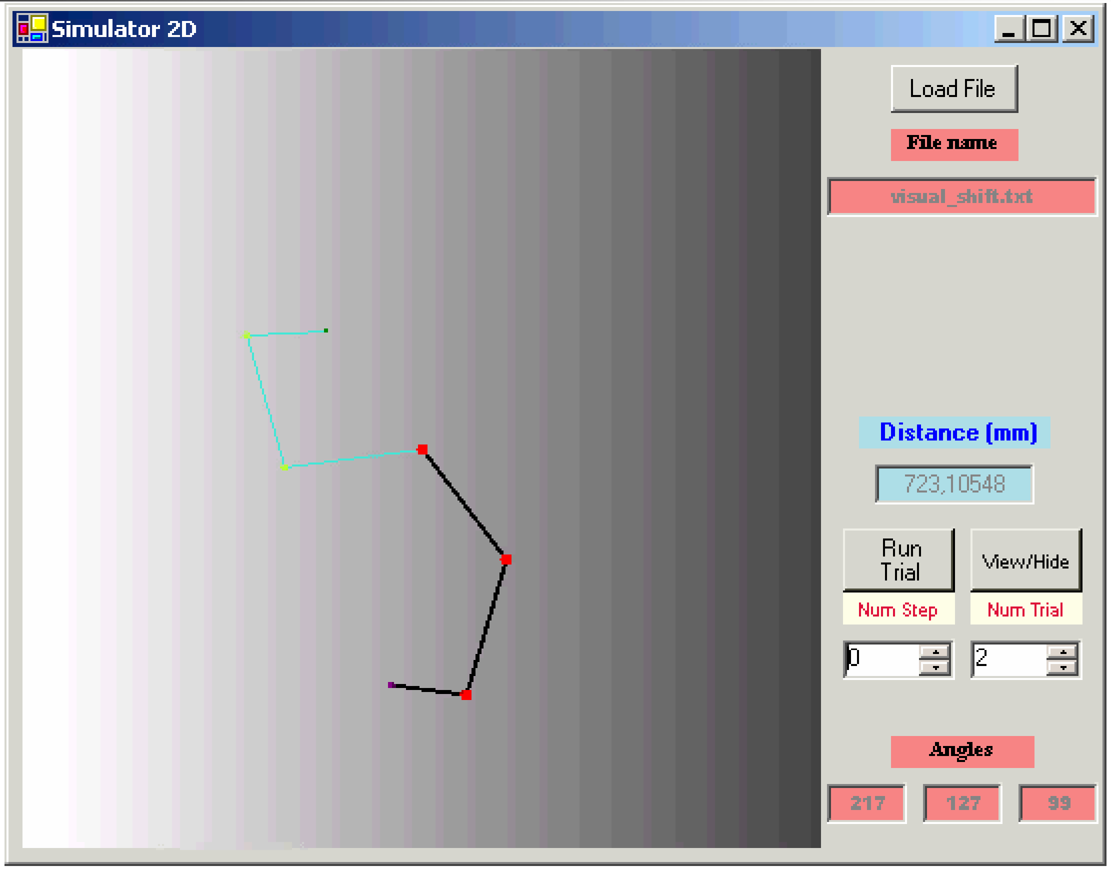

# Experimental results: 2D simulation - blind reaching

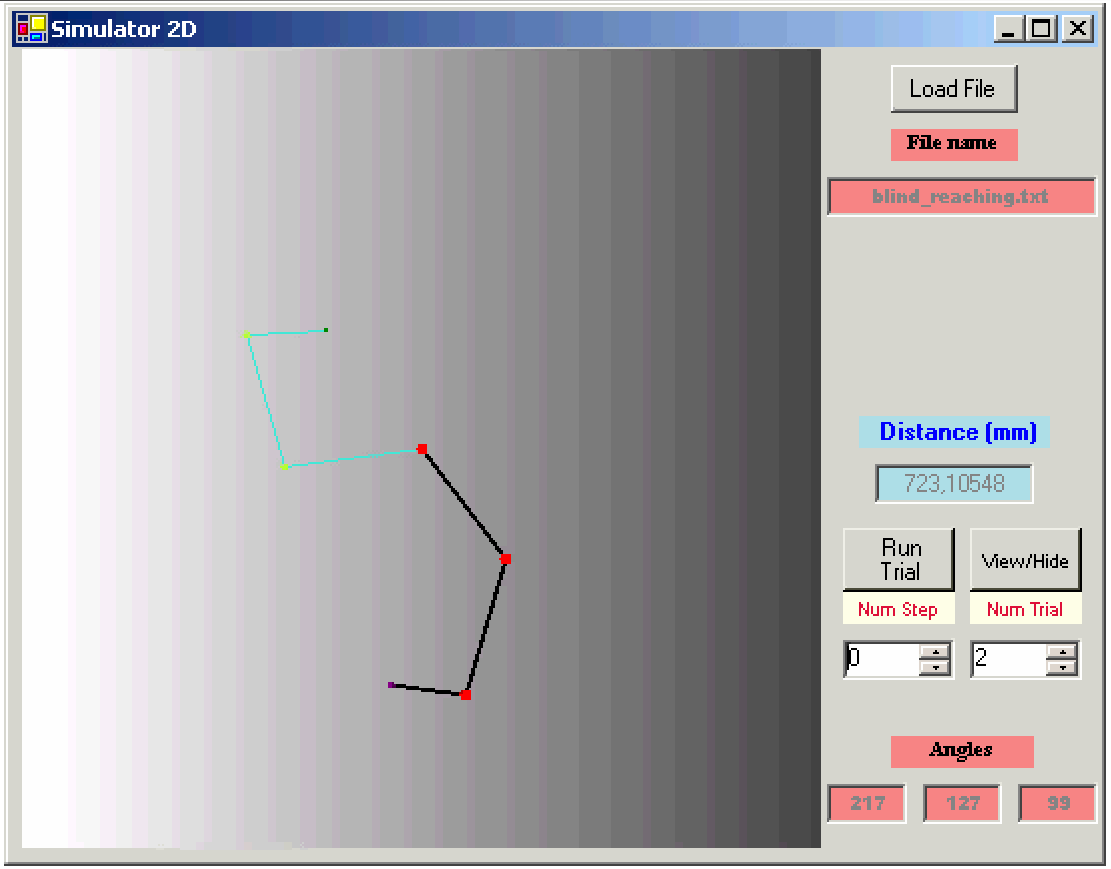

# Experimental results: Dexter Arm

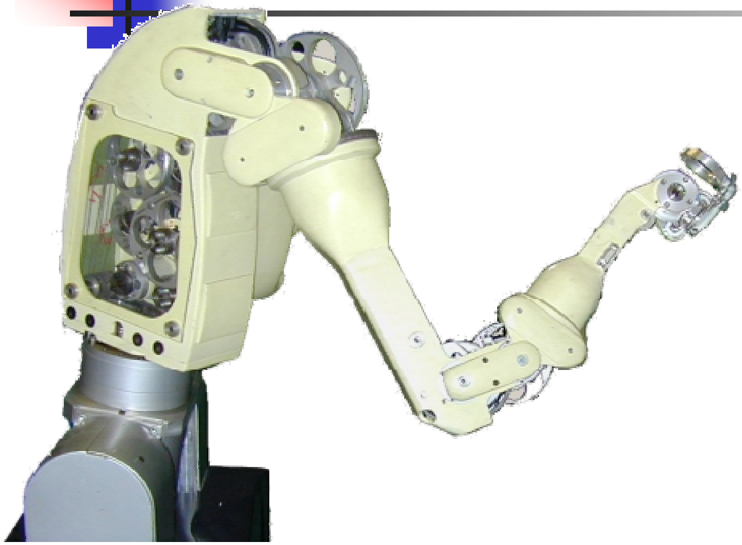

- D.o.f.: 8
- Velocity: 0.2 m/s
- Workspace: 1200 mm x 350°
- Repeatability: ± 1mm
- Weight: 40 Kg
- Payload: 2 Kg
- Power: 24V DC

- 8-d.o.f. anthropomorphic redundant robot arm, composed of trunk, shoulder, elbow and wrist
- mechanically coupled structure: the mechanical transmission system is realized with pulleys and steel cables
- main characteristics: reduced accuracy,lighter mechanical structure, safe and intrinsically compliant structure

# The Dexter Arm

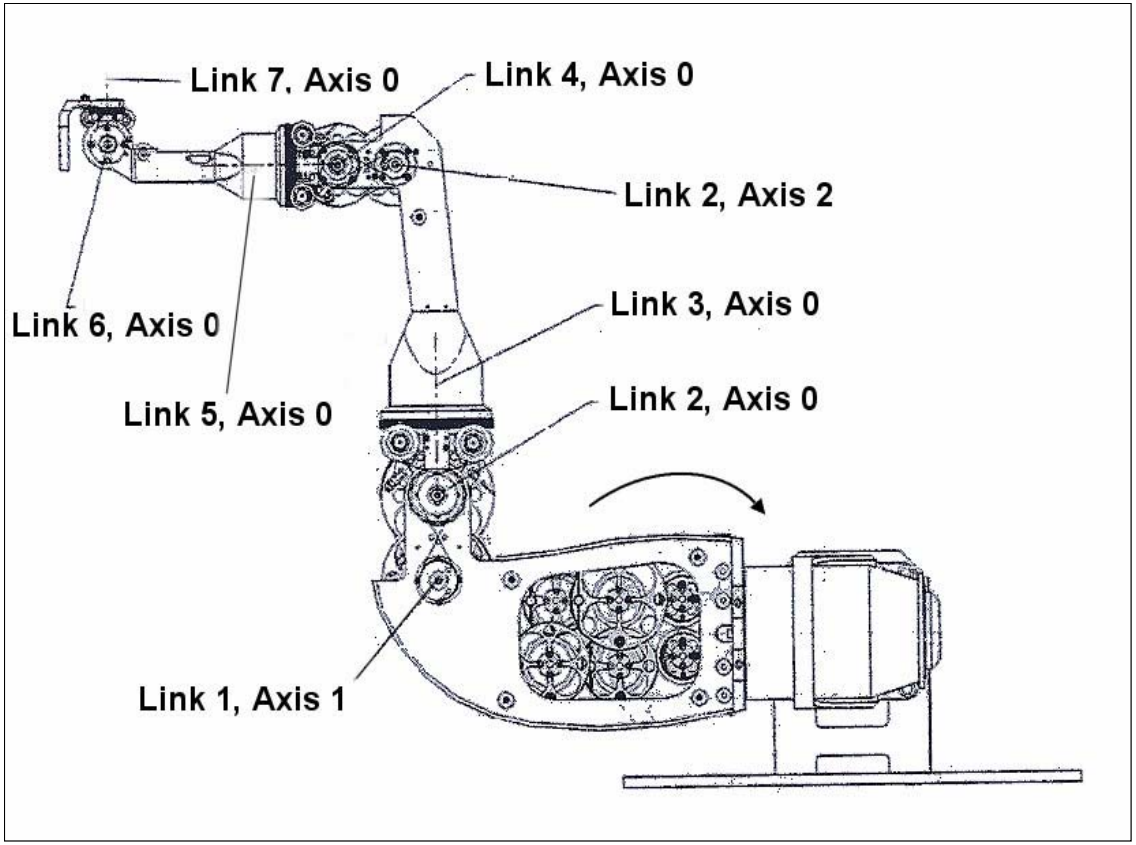

# Simulation of the vision system

- Direct kinematics allows to calculate the spatial position of the end effector position and of the target point expressed in the arm reference frame.
- Gaussian noise is added to the visual input simulating unstructured environmental conditions.

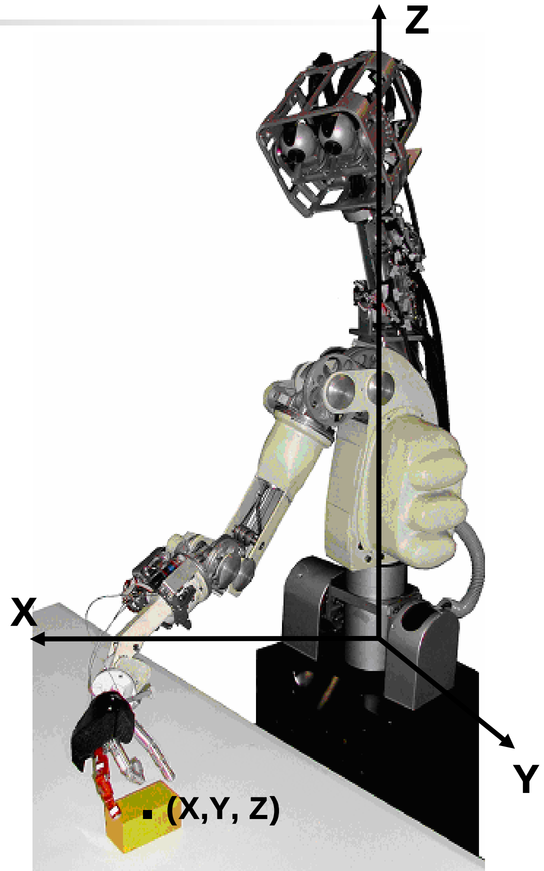

# Training phase

- Through endogenous arm movements, the system generates the associative information needed to build the transformation between a spatial map (which encodes spatial directions) and a motor map (which encodes joint rotations)
- Use of direct kinematics of the arm in order to determine the end effector position in the arm reference system
- 20,511 random movements in the joint space (= number of iterations)
- The GNG map cardinality was 6,883 units

# Testing phase

- After the training phase, given a target 3D point the system provides the joint rotations that drives the current end effector position in the target point
- Five different modalities:
  1. ***normal reaching***
     - without any constraint
  2. ***reaching with a tool***
     - adding a tool of variable length at the end of last link
  3. ***reaching with a clamped joint***
     - reaching tasks with a clamped joint
  4. ***reaching with vision distortion***
     - using a prism that allows a visual shift
  5. ***blind reaching***
     - reaching without using any visual feedback

All trials have been executed **without additional learning**

# Experimental results on the DEXTER robotic arm

# Experimental results on the DEXTER robotic arm

**Distance of the end effector position and of its position from straight line trajectory**

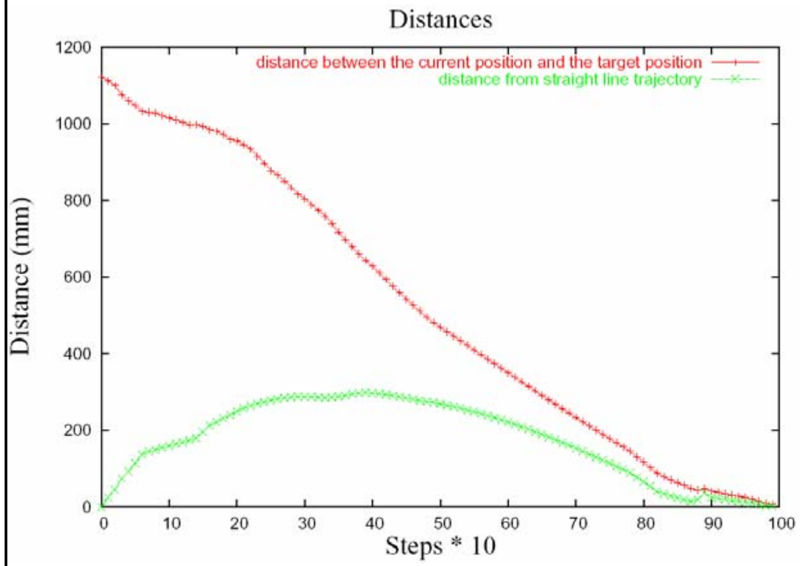


**Joint trajectories**

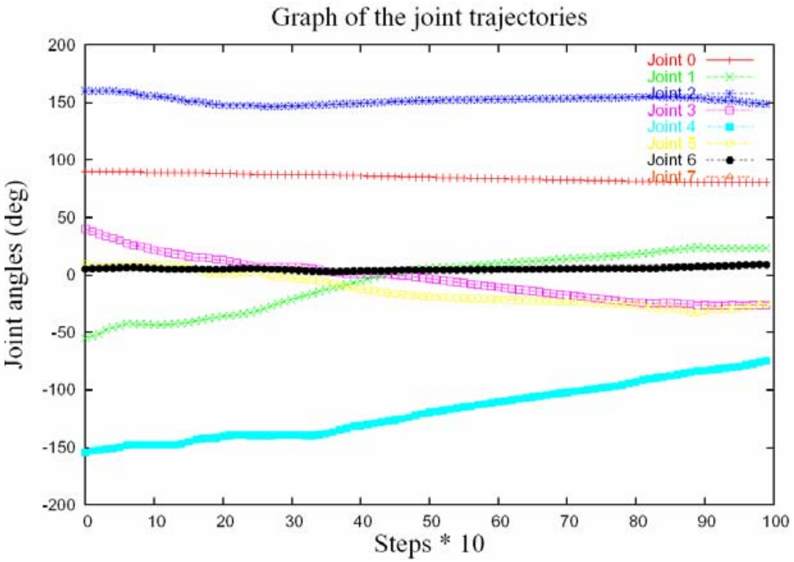

# Experimental results on the DEXTER robotic arm

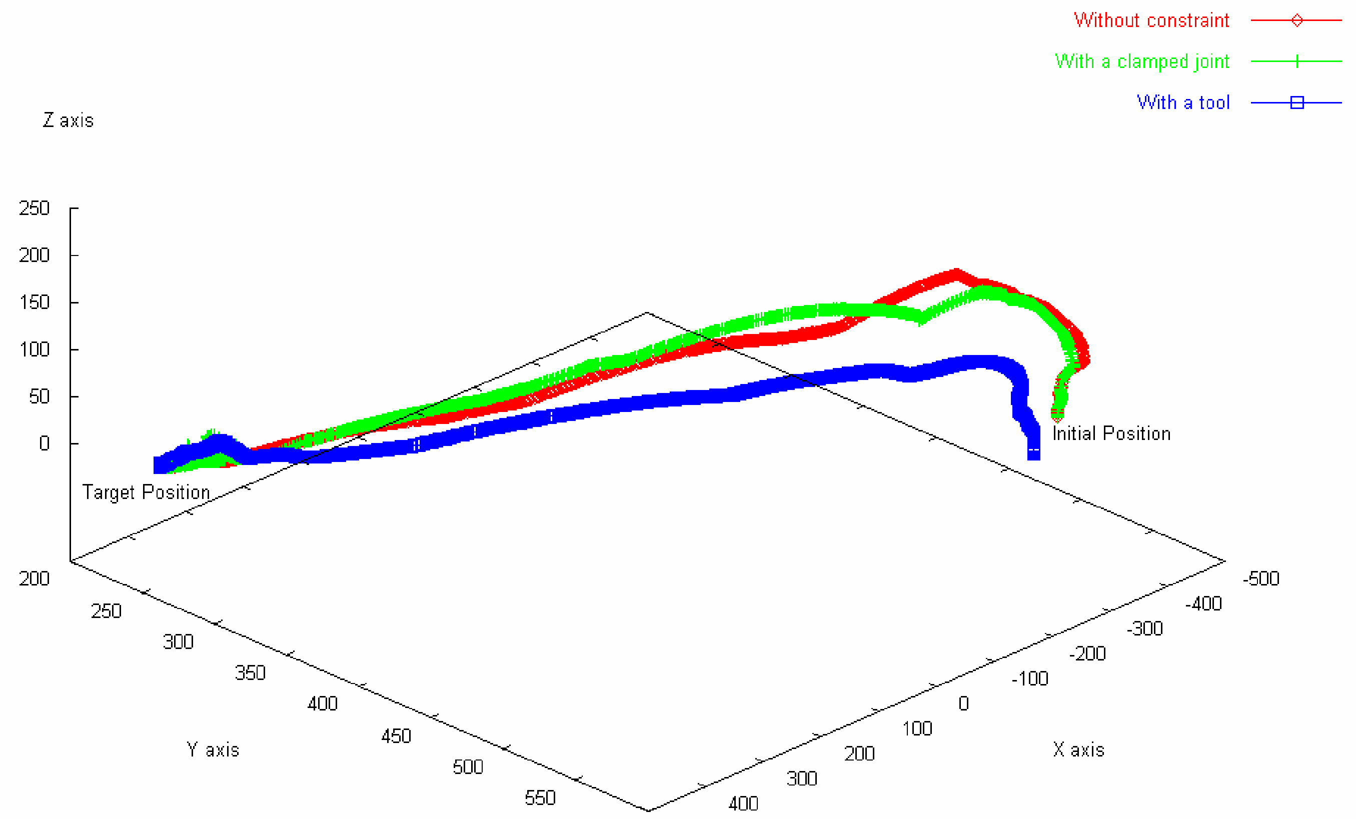

# Experimental results on the DEXTER robotic arm

CLAMPED REACHING

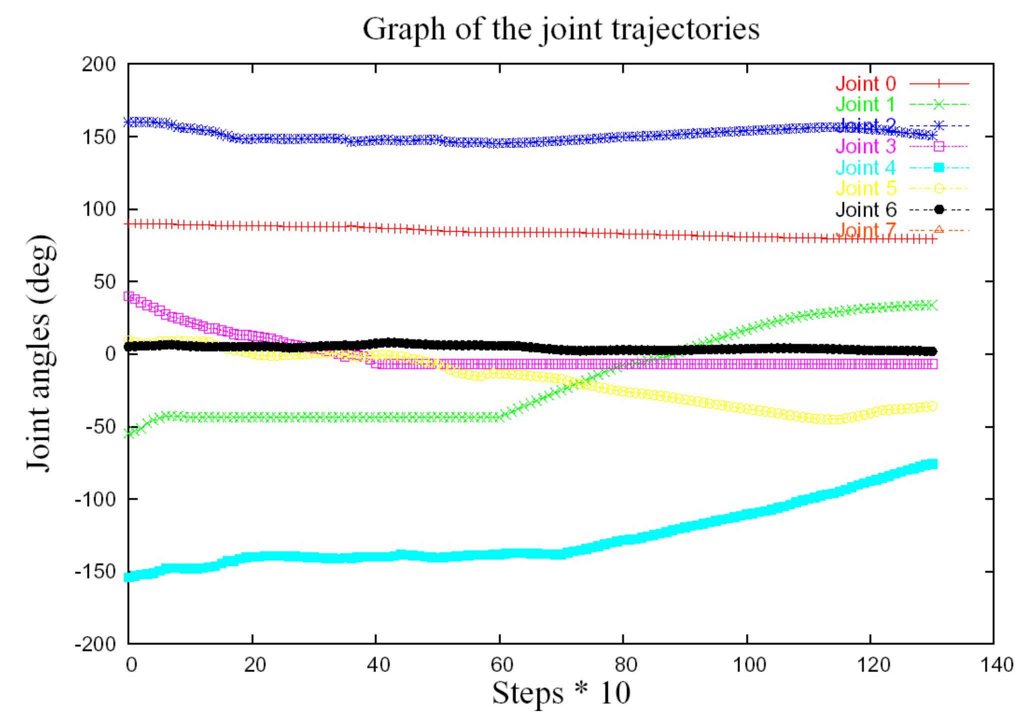

# Experimental results on the DEXTER robotic arm

BLIND REACHING

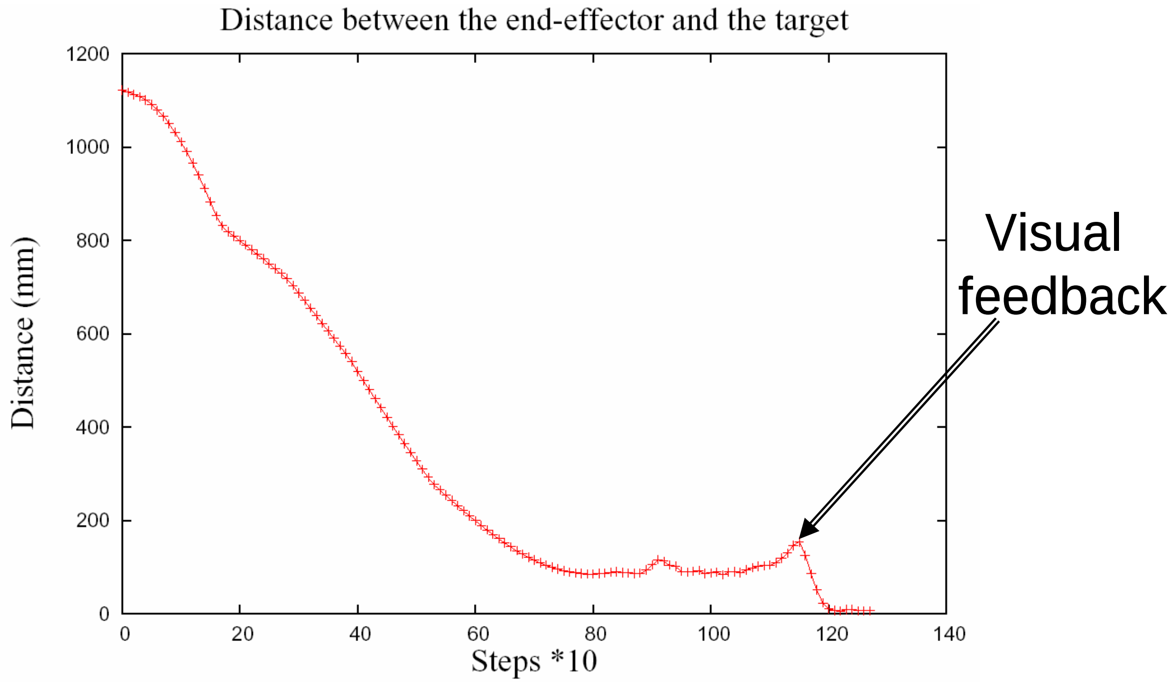

# Experimental results on the DEXTER robotic arm

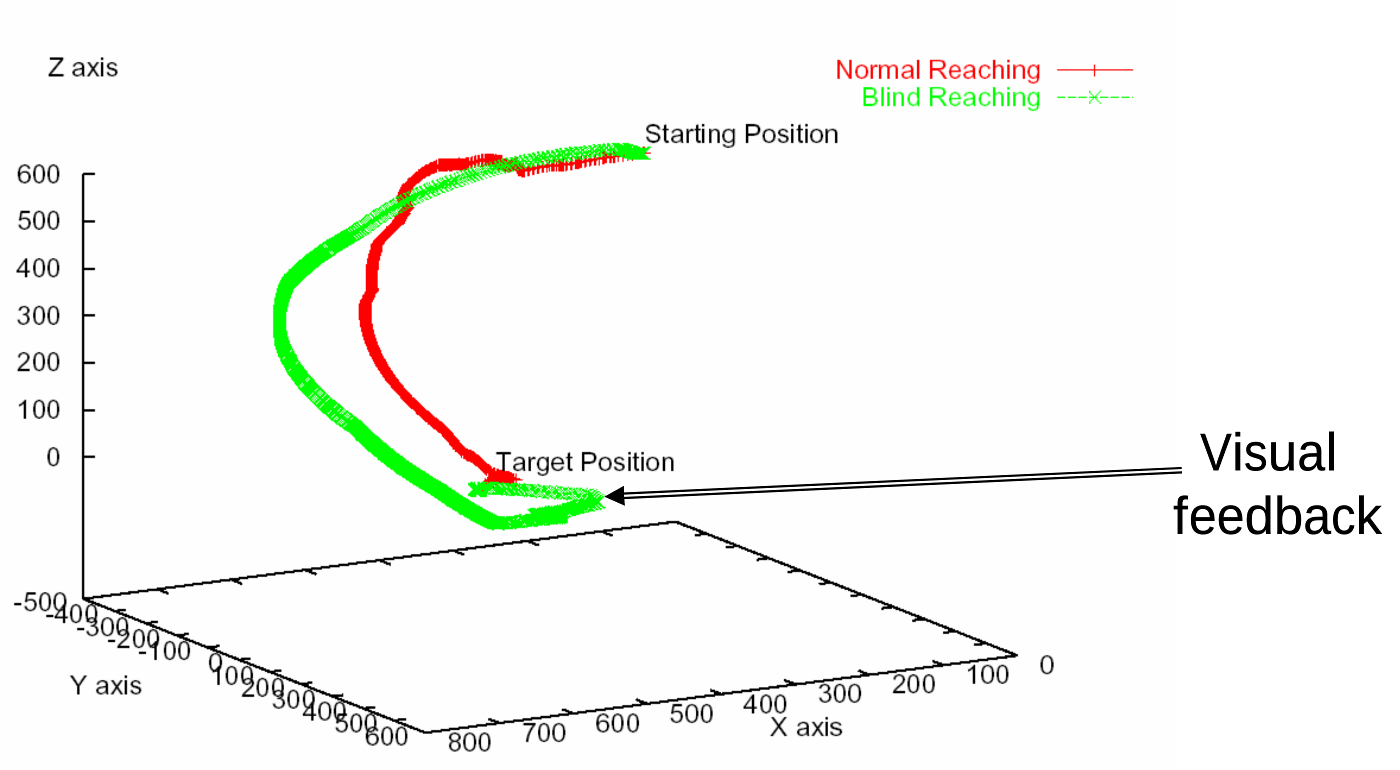

# Experimental results on PUMA 562 robotic arm

# Experimental results on the PUMA 562 robotic arm

**Distance of the end effector position and of its position from straight line trajectory**

**Joint trajectories**

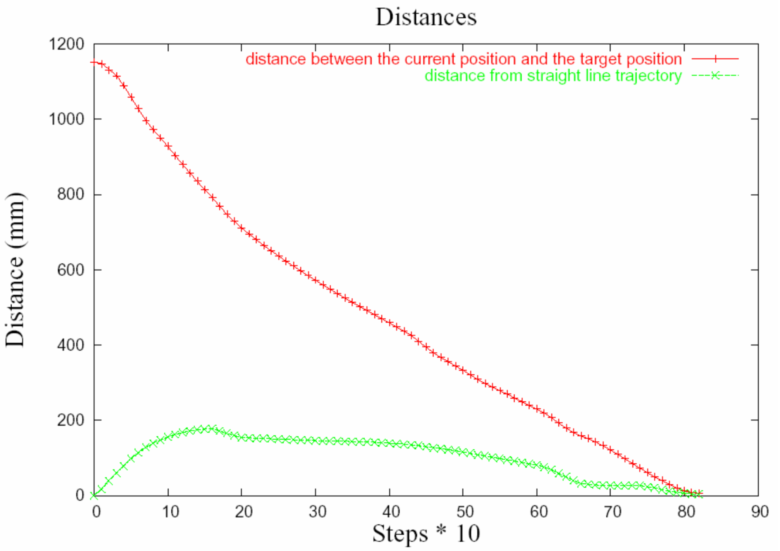


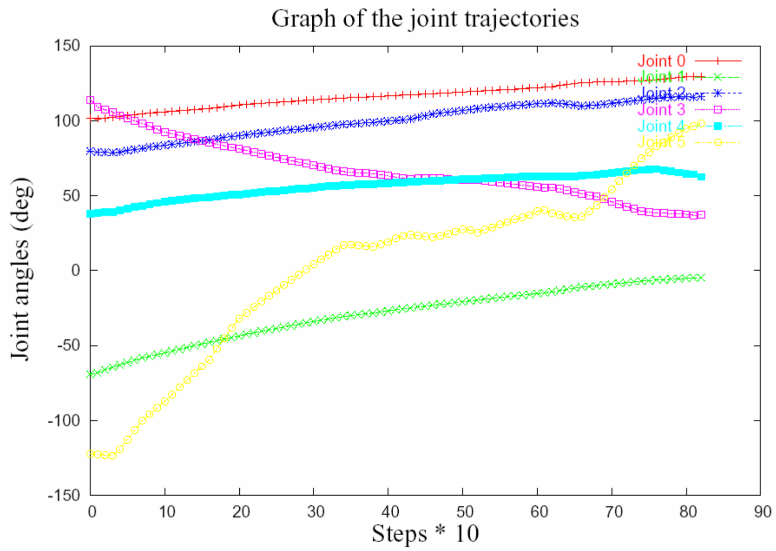

# Experimental results: real robots

NEURAL NETWORK PROPRIETIES

| | Training time (sec.) | # cells of *SMM* | *MQE* Training set | *MQE* Test set |
|---|---|---|---|---|
| **Neuro-robotic platform** | 227 | 6883 | 0.228318 | 0.299936 |
| **PUMA 560** | 16 | 822 | 0.265331 | 0.280599 |

**Pentium IV** (1.8 GHz)

Mean Quantization Error (MQE)

$$\overline{Err\_qnt} = \frac{\sum_{\xi \in \mathcal{A}} \| \xi - \mathbf{w}_{s_1} \|^2}{|\mathcal{A}|}$$

$\mathcal{A}$ is the input data set

$\xi$ is the pattern in input,

$\mathbf{w}_{s1}$ is the reference vector associated to winner unit

# Application of the same approach to different robotic systems

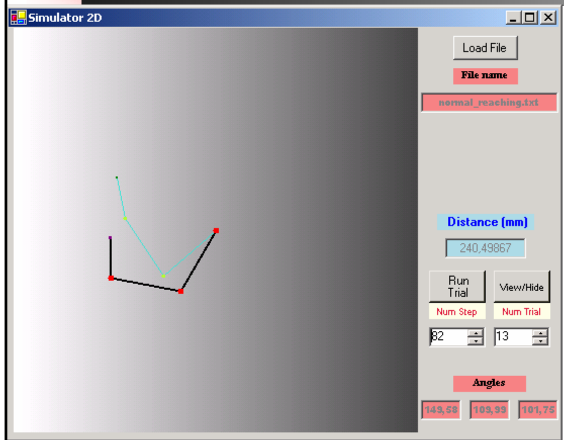


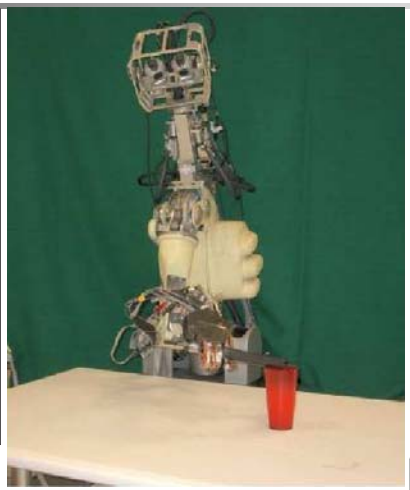

G. Asuni, Leoni F., Starita A., Guglielmelli E., Dario P., "A Neuro-controller for Robot Arms Based on Biologically-Inspired Visuo-Motor Coordination Neural Models", *The 1st International IEEE EMBS Conference on Neural Engineering*, 20 - 22 March, 2003, Capri Island, Italy.

E.Guglielmelli G. Asuni, F. Leoni, A. Starita, P. Dario, "A Neuro-controller for Robot Arms Based on Biologically-Inspired Visuo-Motor Co-ordination Neural Models", *IEEE Handbook of Neural Engineering*, M. Akay (Ed.), IEEE Press, in press (2005).

G. Asuni, G. Teti, C. Laschi, E. Guglielmelli, P. Dario, "A Robotic Head Neuro-controller on Biologically-Inspired Neural Models", *IEEE International Conference on Robotics and Automation* April 18-22, 2005, Barcelona, Spain

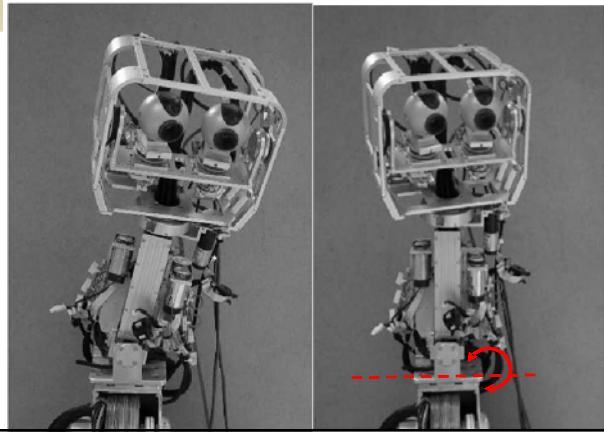

# Addressed Problem

To develop a control module that receives in input a target gaze position and provides in output a command sequence able to reach it

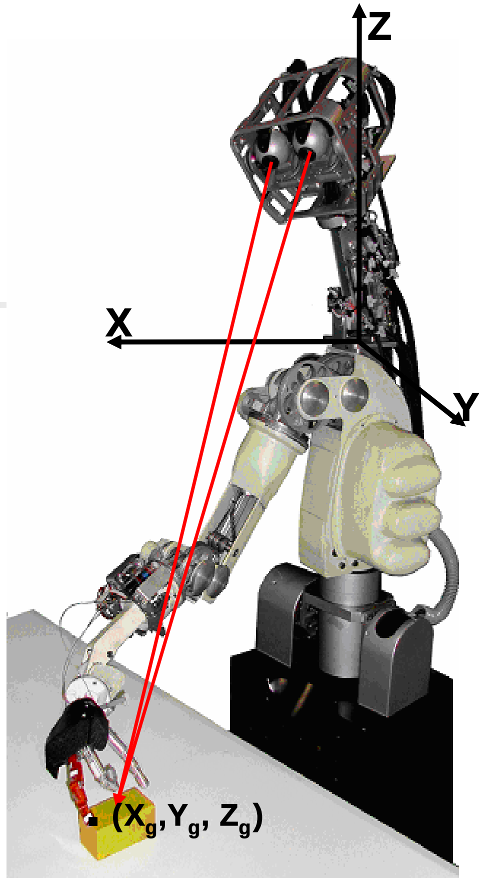


Target Gaze Fixation Point Position $(X_t, Y_t, Z_t)$ → ? → Motor Command $\{(J0_i, \ldots, J6_i)\}$ → HEAD

# The proposed neural model

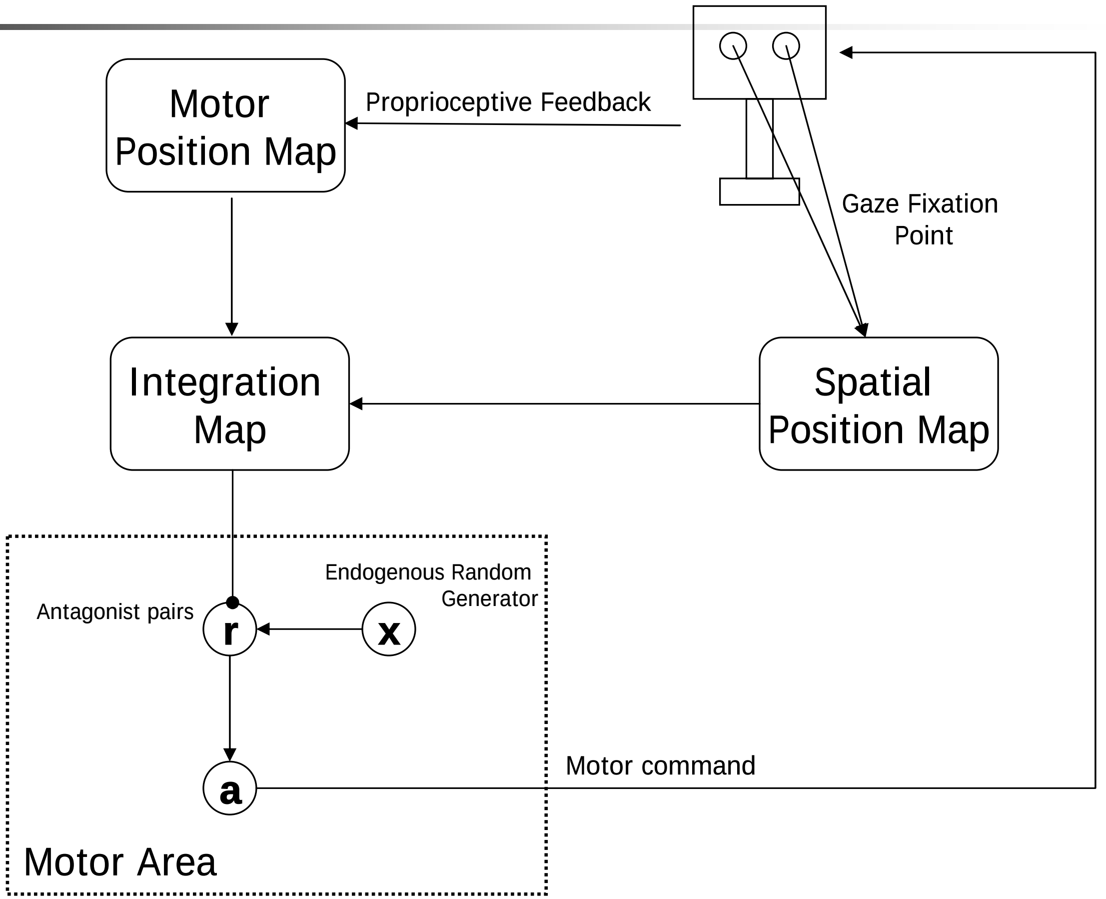

# Testing phase

- After the training phase, given a target fixation point the system provides the joint rotations that drives the current gaze fixation point in the target point

- Three different modalities:
  1. Normal (without any constraint)
  2. With a clamped joint 0
  3. With symmetric angles for eye joints

All trials have been executed without additional learning

# Experimental results: normal gazing

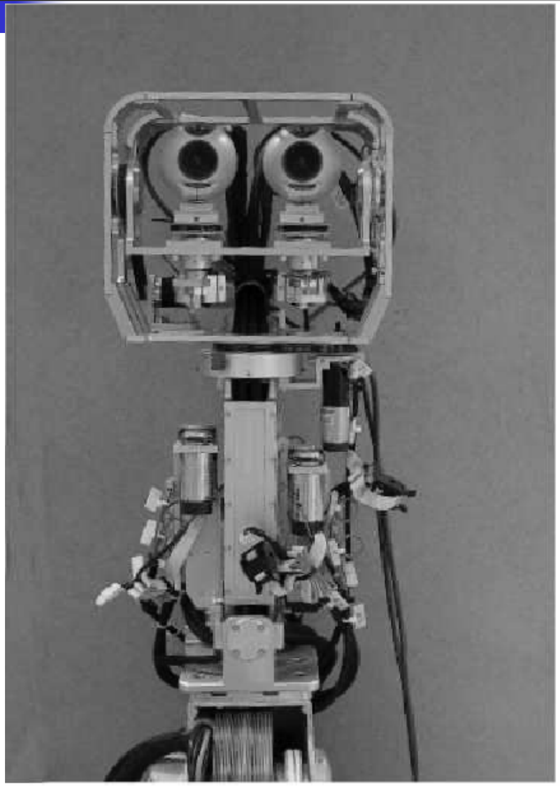

Initial posture

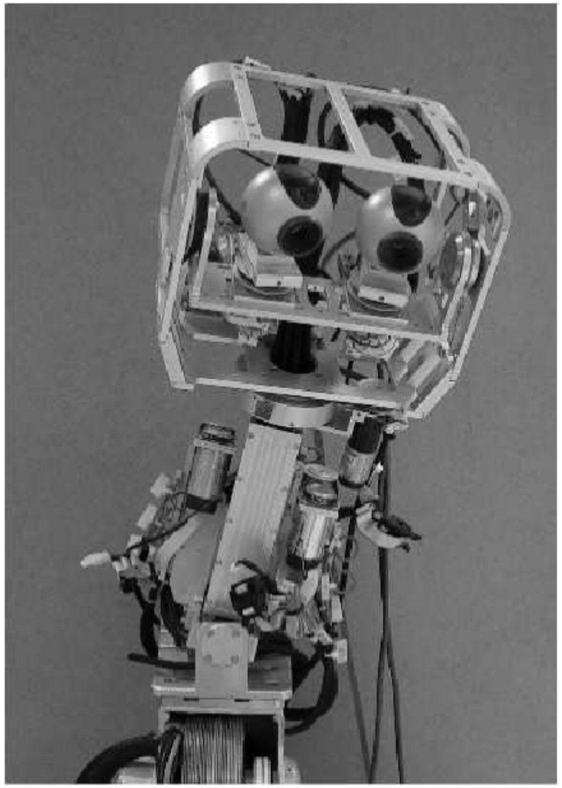

Final posture (normal)

# Experimental results: gazing with a clamped joint

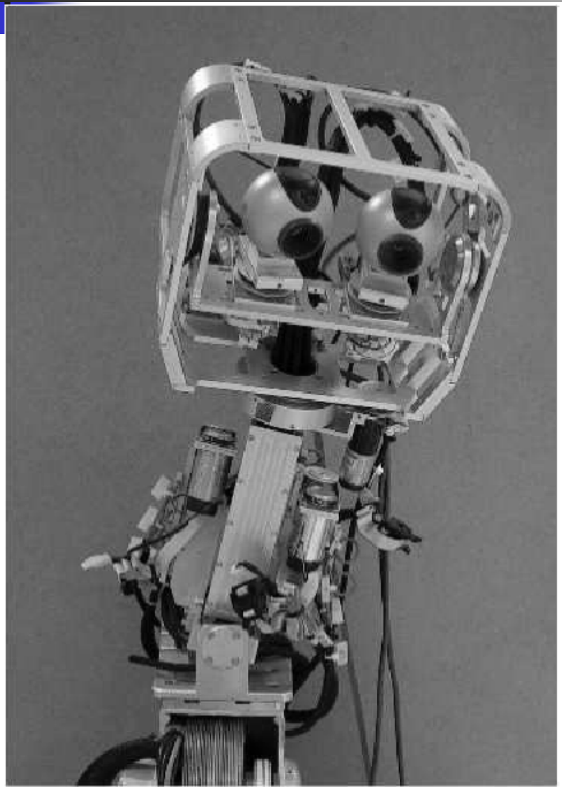

Final posture in normal mode

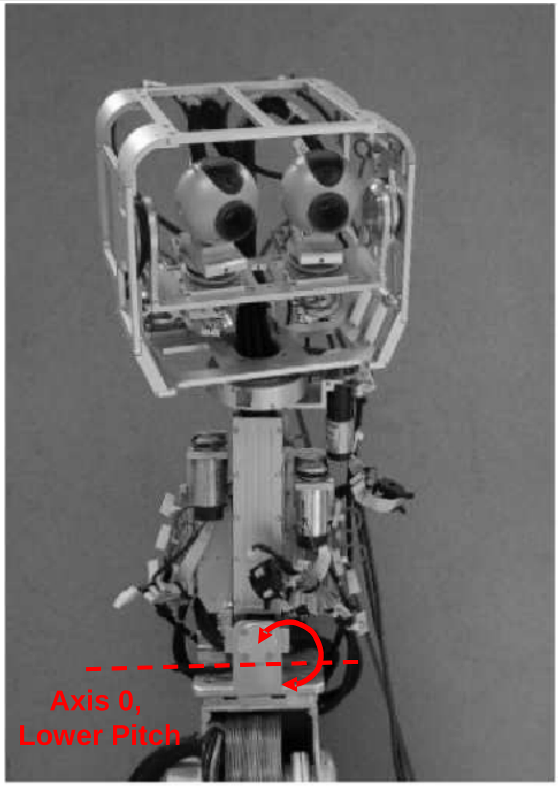


Final posture (clamped joint 0)

# Experimental results: gazing with symmetric eye angles

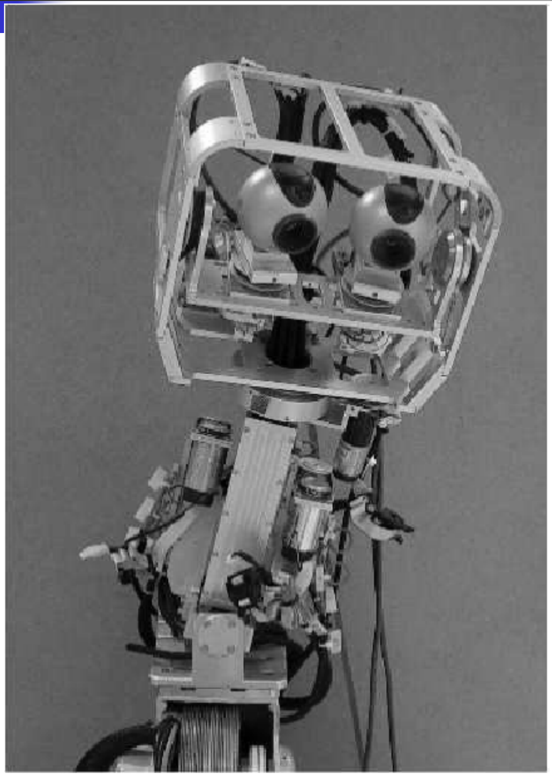

Final posture in normal mode

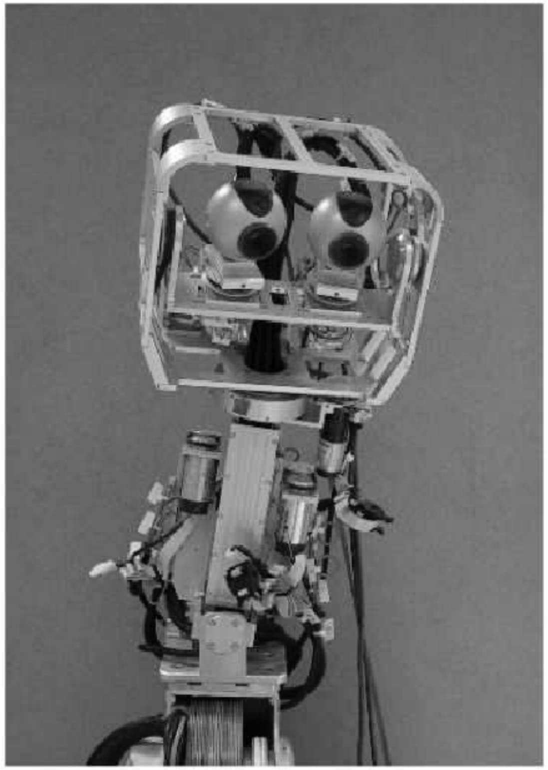

Final posture with symmetric angles for eye joints

# Portability

To allow the portability from a robot system to another it is only needed to:

- change the number of d.o.f.
- for each d.o.f., provide its range of variability

# Future work

- Implementation of continuous learning mechanisms
- Development of an integrated system for the control of the whole upper-body robotic system

# Conclusions

- A basic control scheme for the control of a robotic arm with 8 DOF has been proposed
- Growing Neural Gas networks have been used to implement the model
- With no knowledge about the robotic arm kinematics, after a learning phase, the robot is able to reaching points in the 3D space
- The robot can reach a target point even with additional constraints (e.g. some joints blocked) without additional learning phases
- The neural model has a potential to be able to control different complex robotic systems with no modifications to the model nor to the learning equations